scientific reports

Check for updates

OPEN

Few generalized entropic relations related to Rydberg atoms

Kirtee Kumar[1,2] & Vinod Prasad[3✉]

We calculate the analytical and numerical values of the position space Shannon entropy, momentum space Shannon entropy, and total Shannon entropy, S_ρ, S_γ, and S_T, respectively, of free and trapped Rydberg hydrogen-like atoms. The influence of atomic number Z, the principal quantum number n, and energy E on the Shannon entropy of the Rydberg atoms are illustrated. The scaling properties of Shannon entropy with energy of states E and the principal quantum number n have been reported for the first time to the best of our knowledge. Our work explains how Shannon entropy indicates localization-delocalization of the wavefunction. The total Shannon entropy as a measure of the number of nodes in the trapped Rydberg atom's wavefunction is also discussed. We show why an uncertainty relation based on Shannon entropy is superior to Heisenberg uncertainty for Rydberg atoms.

Rydberg atoms are atoms in which one or more valence electron can be excited in states with extremely high principal quantum numbers n[1,2]. The valence electron is predominantly affected in such an atom by the positive charge of the ionic centre, not by its composition. These atoms that demonstrate the consistency of thought between the world of classical mechanics and quantum mechanics are important to study the correlation of classical and quantum regime. Although the study of Rydberg atoms has a long history, the advancement of laser technology has led to great experimental advances for researchers and has revived interest in such studies. Rydberg atoms are also significant in many research studies of astrophysics. These states in theory, give some advantages that could be exploited in the research for new applications. The special properties of Rydberg atoms, *i.e.*, their extreme polarizability, long-range interaction, and long lifetime, have positioned them at the centres of highly active research areas of modern atomic physics and quantum information technology. In 2000, Jaksch et al. proposed a method of generating a fast phase gate using Rydberg atoms, which was the first proposal to use the blockade for quantum information[3]. It was further extended to a mesoscopic regime of many-atom ensemble qubits[4]. Rydberg blockade and antiblockade has also been suggested as a way to generate many-particle entanglement[5–12]. Carr and Saffman have proposed and analysed an approach for preparation of high fidelity entanglement and anti-ferromagnetic states using Rydberg mediated interaction with dissipation for two atom singlet[13]. It was further extended to a stationary three-dimensional entanglement between two-individual neutral Rydberg atoms[14] and maximally entangled states via dissipative Rydberg pumping[15]. In the excitation spectra of ultra cold atoms of Rubidium and Cesium in their Rydberg states, dipole matrix elements and relevant energies were calculated using quantum defect theory[16]. So, there are many studies related to Rydberg atoms which are promising platform for quantum state engineering, quantum metrology, quantum simulation[17,18], quantum information[21], quantum computing[19,20,22], sensing and imaging and quantum optics[23].

Firstly, Michels et al. introduced the idea of study of confined atom. They studied spectral broading of the hydrogen atom inside an impenetrable spherical cavity[24]. The trapped atoms show enhanced response to external perturbation compare to free atoms. In recently, mostly experiments are performed with Rydberg atoms in optical dipole traps and arrays of optical dipole traps. The atoms are temporarily excited to Rydberg states using resonant laser radiation. Typically, the ground-state atoms are trapped by off-resonant trapping radiation, but Rydberg atoms are not trapped. Rydberg atoms are repelled by the Laser-induced ponderomotive potential[25] and transversely trapped in the light tube for times up to 10 *ms*. The experiments of trapping Rydberg atoms have been reported in recent years[26–32]. The theoretical description of trapped Rydberg atoms and their interaction with light and with each other is commonly performed using conventional quantum mechanical approach based on Schrodinger equation. The trapped Rydberg atoms have more quantum information than the free Rydberg atoms because the free atoms interact only at very short range[33]. The trapped Rydberg atoms open up new possibilities for applications of quantum optics and quantum information[34,35]. Therefore, trapped Rydberg atoms have taken importance in recent studies[36].

[1]Department of Physics and Astrophysics, University of Delhi, Delhi 110007, India. [2]Department of Physics, Motilal Nehru College, University of Delhi, Delhi 110021, India. [3]Department of Physics, Swami Shraddhanand College, University of Delhi, Delhi 110036, India. ✉email: vprasad@ss.du.ac.in

nature portfolio

1

The spread of the probability densities in both position and momentum space determine the physical and chemical properties of the Rydberg atoms. The multiple facets of this spread are currently quantified not only by means of radial expectation values in position and momentum spaces, but also by certain local and global information-theoretical measures. Various fundamental and/or experimentally measurable quantities such as the diamagnetic susceptibility, the potential energy, the kinetic energy, etc. are closely related to these spreading measures. In addition, they allow to determine various uncertainty measures.

There has been continuous interest in the studies on information theoretic measures for quantum mechanical systems. Entropy is a measure of the uncertainty associated with a random variable in information theory. Entropy usually refers to the Shannon entropy in this field, which measures the expected value of the information stored in a message, usually in units such as bits, i.e., when the value of the random variable is unknown, it is a measure of the average information content that is missing. Claude E. Shannon presented this idea in his paper "A Mathematical Theory of Communication" in 1948, in which he set out to find fundamental limits on signal processing operations such as data compression and data storage and communication reliability[37]. In other fields, such as statistical mechanics, cryptography, quantum computing[38], atomic and molecular physics[39–45] and chemistry[46,47], this theory has bee extended to a range of applications since its proposal.

From the underlying concepts of information theory, the global measure of Shannon entropy is fundamental to quantum information-theoretical measures. There are other global measures, besides Shannon entropy, which include Tsallis and Renyi entropies and Onicescu energy[48–51]. The importance of the global measure is to study the uncertainty associated with the distribution of probability[52–55]. An uncertainty relation based on the Shannon entropy known as BBM inequality derived by Beckner-Bialynicki-Birula and Mycieslki[56,57] which is a stronger version of the Heisenberg uncertainty principle of quantum mechanics, which is written as

$$S_T = S_\rho + S_\gamma \geq d(1 + \ln \pi) \tag{1}$$

where, d is the spatial dimension, S_ρ and S_γ are Shannon entropy for position and momentum spaces, which are expressed as

$$S_\rho = -\int \rho\left(\vec{r}\right) \ln \rho\left(\vec{r}\right) d\vec{r} \tag{2}$$

$$S_\gamma = -\int \gamma\left(\vec{p}\right) \ln \gamma\left(\vec{p}\right) d\vec{p} \tag{3}$$

respectively. Where, $\rho(\vec{r})$ and $\gamma(\vec{p})$ are the radial probability density in position and momentum space respectively and they are written as $\rho(\vec{r}) = |\Psi(\vec{r})|^2$ and $\gamma(\vec{p}) = |\Phi(\vec{p})|^2$, where $\Psi(\vec{r})$ and $\Phi(\vec{p})$ are the normalized wave function in position and momentum space respectively. One of the implications of the BBM inequality is that the lower bound values of the Shannon entropy sum are interpreted in such a way that if the position entropy increases, the momentum entropy will decrease in such a way that its sum follows the bound of BBM inequality. In physical science, Shannon entropy is a hypothesis that describes the spatial distribution of the wave function for different states. The concentration of wave function of the state is higher when the Shannon entropy is small[58]. We may also assume that the wavefunction is localized when the Shannon entropy is low and delocalized when it is high. As a consequence, Shannon entropy can be used to estimate the stability of a system. When Shannon entropy is low, it is likely to be more stable, and when Shannon entropy is high, it is assumed to be unstable. Shannon entropy is also important in the study of the structure and dynamics of atomic and molecular systems since it is related to fundamental and experimentally observable quantities like kinetic energy and magnetic susceptibility[59]. Shannon entropy has attracted a lot of attention due to its application in different fields. Saha and Jose use Shannon entropy as an indicator of correlation and relativistic effects in confined atoms[60]. Recently, many researchers have used various potentials to study the Shannon entropy[61–64]. Shannon entropy for quantum heterostructures has also been studied[65–67]. The Shannon entropy of the confined hydrogenic atoms have been calculated in many previous works[68–71]. Very recently, there are studies on the influence of electric field on the Shannon entropy[72,73]. As a result, we intend to investigate the analytical and numerical calculation of Shannon entropy and various entropic uncertainty relations[74–78] for the Rydberg hydrogen atom, as suggested in the work's concept.

Method

The non-relativistic Hamiltonian of a Hydrogen-like atom of mass M and atomic number Z with the nucleus placed in the center of an impenetrable sphere is

$$H = \frac{p^2}{2M} - \frac{Ze^2}{r} + V_c(r) \tag{4}$$

where e is the charge of electron and $V_c(r)$ is the spherical hard confining potential which is written as

$$V_c(r) = \begin{cases} 0 & \text{for } r \leq r_0 \\ \infty & \text{for } r > r_0 \end{cases} \tag{5}$$

Where r_0 is the radius of spherical confinement.

Using $p = -\iota\hbar\nabla$, Hamiltonian becomes

$$H = \frac{-\hbar^2 \nabla^2}{2M} - \frac{Ze^2}{r} + V_c(r) \tag{6}$$

Using atomic unit (a.u.) ($\hbar = 1$, $M = 1$ and $e = 1$), Hamiltonian can be written as

$$H = \frac{-\nabla^2}{2} - \frac{Z}{r} + V_c(r) \tag{7}$$

So, the Schrodinger equation $H\Psi = E\Psi$ is written as

$$\left(\frac{-1}{2}\nabla^2 - \frac{Z}{r}\right)\Psi = E\Psi \tag{8}$$

In spherical coordinates the Schrodinger equation is written as

$$\frac{-1}{2}\left[\frac{1}{r^2}\frac{\partial}{\partial r}\left(r^2\frac{\partial \Psi}{\partial r}\right) + \frac{1}{r^2 \sin\theta}\frac{\partial}{\partial \theta}\left(\sin\theta\frac{\partial \Psi}{\partial \theta}\right) + \frac{1}{r^2 \sin^2\theta}\left(\frac{\partial^2 \Psi}{\partial \phi^2}\right)\right] - \frac{Z}{r}\Psi = E\Psi \tag{9}$$

Because of spherical symmetry the above Schrodinger equation can be solved by the method of separation of variables. So, complete normalized wavefunction $\Psi_{nlm}(r, \theta, \phi)$ can be written as

$$\Psi_{nlm}(r, \theta, \phi) = R_{nl}(r)Y_{lm}(\theta, \phi) \tag{10}$$

where, $R_{nl}(r)$ represents the radial part and $Y_{lm}(\theta, \phi)$ is the angular part of the wavefunction. The angular part of wavefunction $Y_{lm}(\theta, \phi)$ is same and radial part $R_{nl}(r)$ is affected due to confining potential. So, the radial Schrodinger equation can be written as

$$\frac{d}{dr}\left(r^2\frac{dR_{nl}(r)}{dr}\right) - 2r^2\left[-\frac{Z}{r} + \frac{l(l+1)}{2r^2} - E\right]R_{nl}(r) = 0 \tag{11}$$

Using $R_{nl}(r) = \frac{\xi_{nl}(r)}{r}$, the radial equation finally reduces to the following form

$$\frac{-1}{2}\frac{d^2\xi}{dr^2} + V_{eff}\xi = E\xi \tag{12}$$

where, V_{eff} is effective potential which is defined as $V_{eff} = -\frac{Z}{r} + \frac{l(l+1)}{2r^2}$.

For given effective potential, Eq. (12) is solved numerically by 9th order finite difference method using MATLAB. The eigenvalues equation for radial Schrodinger equation is reduced to a matrix form. Diagonalizing this matrix the eigenvalues and eigenvectors are obtained. So, radial wavefunctions $R_{nl}(r)$ are obtained in position space using these eigenvectors. So, total normalized wavefunction $\Psi_{nlm}(\vec{r}) = R_{nl}(r)Y_{lm}(\theta, \phi)$ can written in position space. Using Dirac-Fourier transformation, the momentum space wavefunction of the position space wavefunction can be written as

$$\Phi(\vec{p}) = \frac{1}{(2\pi)^{\frac{3}{2}}}\int e^{-\iota \vec{p} \cdot \vec{r}}\Psi(\vec{r})d\vec{r} \tag{13}$$

Using $\Psi(\vec{r})$ and $\Phi(\vec{p})$, we obtain probability density $\rho(\vec{r}) = |\Psi(\vec{p})|^2$ in position space and $\gamma(\vec{p}) = |\Phi(\vec{p})|^2$ in momentum space respectively. From $\rho(\vec{r})$ and $\gamma(\vec{p})$, we calculate the Shannon entropy S_ρ in position space and the Shannon entropy in momentum space S_γ respectively, which are presented in next section.

Results and discussion

In the present work, we studied the differences in Shannon entropy between free Rydberg atoms and confined (trapped) Rydberg atoms. The study is limited to the S states with zero angular momentum ($l = 0$), which are known as linear states. As a model, we considered a spherical trapping potential with infinite wells. We have used atomic units throughout this paper.

Free linear Rydberg states. In Table 1, we have presented the values of the Shannon entropy in position space S_ρ, the Shannon entropy in momentum space S_γ, Heisenberg uncertainty principle (HUP) and uncertainty relation based on the Shannon entropy ($S_T = S_\rho + S_\gamma$) with atomic number Z for $n \geq 6$ for s-states of Hydrogen-like atoms. We note that as the atomic number Z increases while the principal quantum number n remains constant, the energy becomes more negative, implying that the energy decreases as Z increases. The nucleus has a more positive charge as Z increases, so the coulombic attraction force between the nucleus and electron increases, causing the nucleus to hold the electron tighter. The energy becomes less negative as n is raised while holding Z unchanged, showing that energy increases as n is raised. It is because of increasing of n, the distance between the nucleus and electron increases so the coulombic attraction force between the nucleus and electron decreases, due to this nucleus holds the electron less tight. As Z increases while n remains constant, potential energy becomes more negative, meaning that potential energy decreases as kinetic energy rises. As Z increases, the wavefunction of the electron compresses in position space and expands in momentum space, resulting in a wavefunction that is localized in position space but delocalized in momentum space. However, we know that as n increases while Z remains constant, the distance between the nucleus and electron increases, therefore potential energy becomes less negative, meaning that potential energy increases and kinetic energy decreases. As n

3

increases, the wavefunction of the electron expands in position space and contracts in momentum space, resulting in wavefunction delocalization in position space and localization in momentum space, as shown in Fig. 1. Standard deviation and Shannon entropy can also be used to explain this. With principal quantum number n and atomic number Z, we observed the variation of variance in position space Δr and variance in momentum space Δp. Keeping n constant, Δr decreases for increasing of Z and Δp increases for increasing of Z. However, if Z remains unchanged, Δr increases as n increases, and Δp decreases as n increases. This also shows that the wavefunction in position space becomes localized and delocalized in momentum space as Z increases (while holding n constant), and vice versa. Here, we can also notice that product of variance $\Delta r \Delta p$ is independent with Z and equal for all values of Z, but it depends on n and increases for increasing of n. Now we can see how Shannon entropy changes with principal quantum number n and atomic number Z in linear Rydberg states. Rosa et al. derived and analyzed the expressions for entropy and complexity of linear Rydberg states of Hydrogenic atoms[79]. Yanez et al. obtained the analytical results for the S_T of free H-like atoms[80,81]. The scaling properties of Shannon entropy with atomic number Z were also discussed in previous works[82,83]. Guevara et al.[84] obtained S_ρ and S_γ as a function atomic number Z for the ground state of H-like atoms and have made an interesting observation that total Shannon entropy S_T is independent of Z within the series and that for the ground state 1s the Shannon entropy for position space and momentum space are, respectively given by

$$S_\rho = \ln \pi - 3 \ln Z + 3 \tag{14}$$

$$S_\gamma = 5 \ln 2 + 2 \ln \pi + 3 \ln Z - \frac{10}{3} \tag{15}$$

We use ns states position space wavefunction of the Hydrogen-like atom and obtain the corresponding momentum space wavefunction using Dirac-Fourier transformation (Eq. (13)) and obtain S_ρ and S_γ using Eq. (2) and (3) as a function of principal quantum number n and atomic number Z for free system, respectively can be defined as

$$S_\rho(n,Z) \approx \frac{23}{4} \ln n + \ln \pi - 3 \ln Z + 3 \tag{16}$$

$$S_\gamma(n,Z) \approx -\frac{15}{4} \ln n + 5 \ln 2 + 2 \ln \pi + 3 \ln Z - \frac{10}{3} \tag{17}$$

Summing Eqs. (16) and (17) and we get total Shannon entropy

$$S_T \approx 2 \ln n + 5 \ln 2 + 3 \ln \pi - \frac{1}{3} \tag{18}$$

which is not affected by the value of Z. Thus, in a one-electron atomic structure, S_T is a function of the principal quantum number n rather than the atomic number Z. Now that we've gone over our numerical result from Table 1, we can see that S_T remains constant as Z changes (while keeping principal quantum number n constant) and that S_T increases as principal quantum number n increases. As a result, our results satisfy the Z and n dependency described by Eq. (18). We've found that S_T follows the bound of the BBM inequality, which is defined by Eq. (1). Shannon entropy in position space S_ρ and Shannon entropy in momentum space S_γ numerical values satisfied the analytical values of S_ρ (Eq. (16)) and S_γ (Eq. (17)) for all values of Z and n. Shannon entropy in position space S_ρ decreases while in momentum space S_γ increases for increasing of Z holding n constant. But, S_ρ increases for increasing of n and S_γ decreases for increasing of n holding Z constant. Increasing Shannon entropy denotes wavefunction delocalization (wavefunction expansion), while decreasing Shannon entropy denotes wavefunction localization (wavefunction compression). As a conclusion of our results, we can state that the wavefunction in position space is localized while wavefunction in momentum space becomes delocalize as Z increases (while n remains constant), and vice versa as n increases (while Z remains constant). Figures 1 and 2 represent the variance of the wavefunction and electron probability density in position space as a function of r with Z and n, respectively, demonstrating that raising Z compresses both the wavefunction and the electron probability density while increasing n expands both.

Now, using Eqs. (16) and (17), and logarithmic operation $\log_n M = \log_n b \times \log_b M$, the variation (difference) in S_ρ and S_γ for cases of the atomic number (a) Z_1, (b) Z_2 (holding n constant) can be written as

$$S_\rho(Z_2) - S_\rho(Z_1) = \delta S_\rho(Z) = -3X \ln 2 \approx -2.08X \tag{19}$$

$$S_\gamma(Z_2) - S_\gamma(Z_1) = \delta S_\gamma(Z) = 3X \ln 2 \approx 2.08X \tag{20}$$

where, $X = \log_2(Z_2/Z_1)$.

From Eqs. (19) and (20), we conclude that the variation of Shannon entropy with Z is independent to principal quantum number n and depends only to Z_2/Z_1 and also observes that the variation of Shannon entropy in position space S_ρ with Z is equal to negative of the variation of Shannon entropy in momentum space S_γ with Z for constant n ($\delta S_\rho(Z) = -\delta S_\gamma(Z) \approx -2.08X$). Negative sign of $\delta S_\rho(Z)$ shows that S_ρ decreases with increasing of Z and positive sign of $\delta S_\gamma(Z)$ show that S_γ increases with increasing of Z. So, we can say that raising Z compresses the wavefunction in position space while expands wavefunction in momentum space in the same ratio. Due to this, total Shannon entropy S_T remains constant with changing in Z for constant n. As a result, despite the compression of electron probability density, total Shannon entropy S_T remains constant with a rise in Z for constant n, as Sen observed for the ground state Hydrogen-like atoms[85]. In Table 2, Z_1 and Z_2 are to indicate the atomic

States	Z	E	Δr	Δp	S_ρ	S_γ	$\Delta r \Delta p$	$S_T = S_\rho + S_\gamma$
6s	0.5	− 0.003472	36.328316	0.101017	16.486441	− 6.52921	3.669771	9.957207
	1.0	− 0.0139	18.171143	0.201978	14.40713	− 4.449904	3.671383	9.957226
	2.0	− 0.056	9.080299	0.404376	12.327846	− 2.370805	3.671852	9.957041
	3.0	− 0.125	6.084213	0.603411	11.111565	− 1.154556	3.671281	9.957009
	4.0	− 0.222	4.541914	0.80906	10.248586	− 0.291635	3.674681	9.956951
7s	0.5	− 0.002551	49.576747	0.086018	17.3767	− 7.016642	4.264505	10.360058
	1.0	− 0.010204	24.790471	0.172067	15.297386	− 4.93739	4.265616	10.359996
	2.0	− 0.040816	12.388781	0.344528	13.218098	− 2.858331	4.268286	10.359767
	3.0	− 0.091837	8.255441	0.517394	12.001818	− 1.641522	4.271314	10.360296
	4.0	− 0.163265	6.191006	0.690437	11.138845	− 0.778891	4.2745	10.359954
8s	0.5	− 0.001953	64.581759	0.075439	18.149252	− 7.434644	4.871981	10.714608
	1.0	− 0.007812	32.273913	0.151015	16.06995	− 5.355824	4.873848	10.714126
	2.0	− 0.03125	16.137925	0.302288	13.99062	− 3.275737	4.878308	10.714883
	3.0	− 0.070312	10.752641	0.45413	12.774206	− 2.05662	4.883101	10.717586
	4.0	− 0.125	8.062925	0.60621	11.911413	− 1.197129	4.887825	10.714284
9s	0.5	− 0.001543	81.536051	0.067328	18.83181	− 7.803804	5.489621	11.028006
	1.0	− 0.006173	40.760914	0.134755	16.752463	− 5.725004	5.492741	11.027459
	2.0	− 0.024691	20.372147	0.269904	14.673131	− 3.64287	5.498518	11.030261
	3.0	− 0.056	13.582061	0.405377	13.45688	− 2.427931	5.505855	11.028949
	4.0	− 0.098765	10.183177	0.541329	12.593905	− 1.564951	5.512452	11.028954
10s	0.5	− 0.00125	100.515588	0.060827	19.443195	− 8.130654	6.1141	11.312541
	1.0	− 0.005	50.242804	0.121765	17.363776	− 6.050467	6.117807	11.313309
	2.0	− 0.02	25.113544	0.24398	15.284466	− 3.971259	6.127203	11.313207
	3.0	− 0.045	16.740561	0.366513	14.068172	− 2.754818	6.135626	11.313302
	4.0	− 0.08	12.552185	0.489656	13.205204	− 1.892796	6.146249	11.312408

Table 1. The variation of Energy E, variance in position space Δr, variance in momentum space Δp, Shannon entropy in position space S_ρ, Shannon entropy in momentum space S_γ, Heisenberg uncertainty principal $\Delta r \Delta p$ and uncertainty relation based on entropy $S_T = S_\rho + S_\gamma$ with atomic number Z and principal quantum number n for Rydberg linear states of free Hydrogen-like atoms.
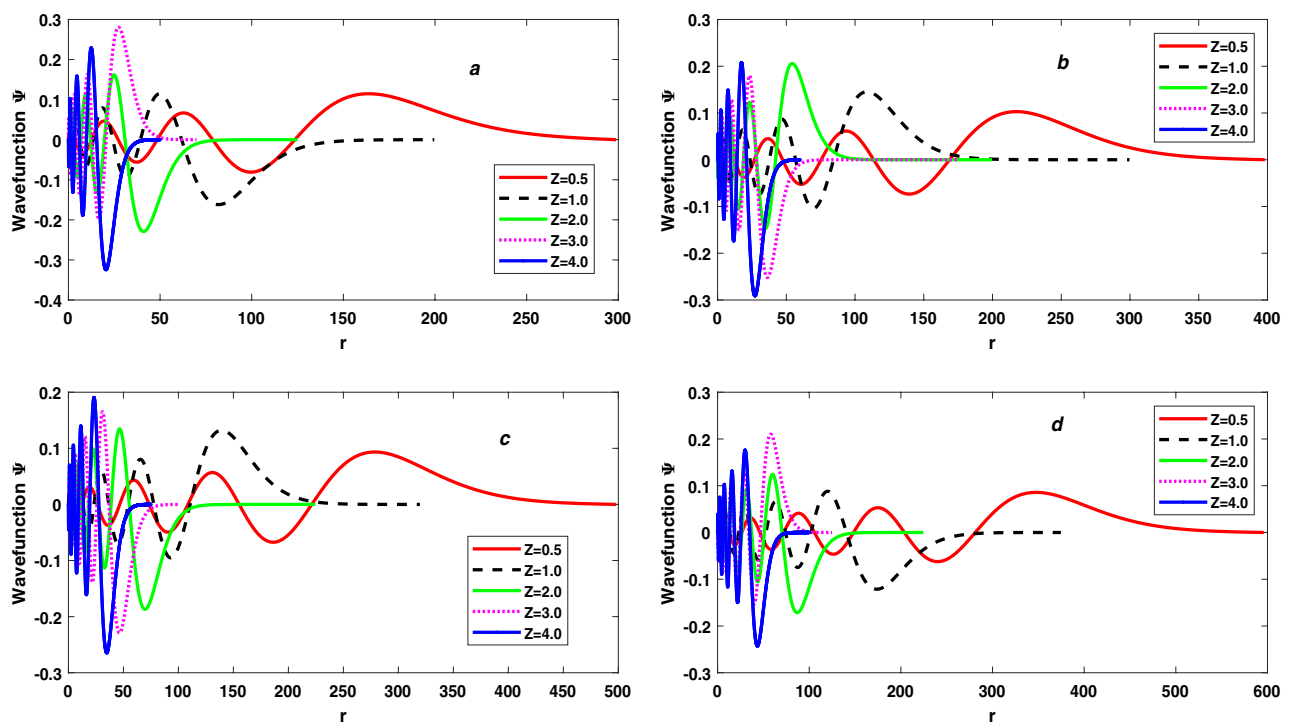
Figure 1. The variation of Wavefunction Ψ with r and atomic number Z for 7s state (**a**), 8s state (**b**), 9s state (**c**) and 10s state (**d**) of free Hydrogen-like atoms.
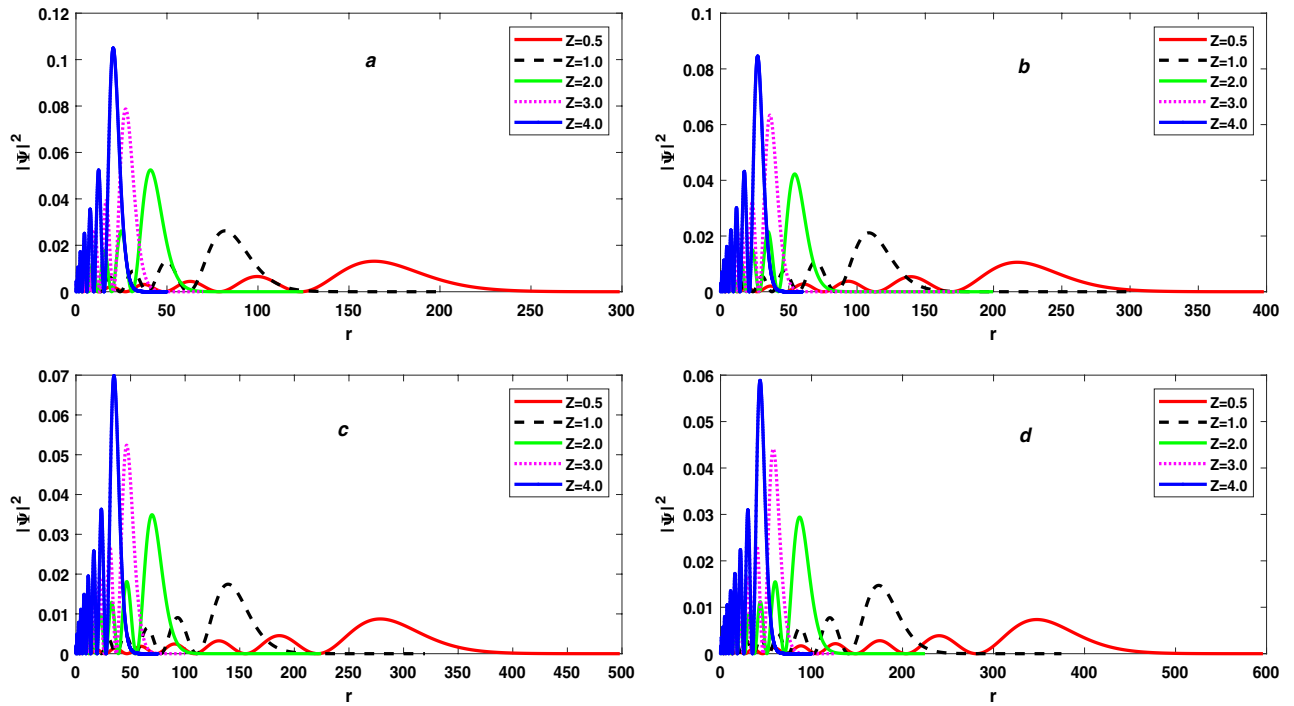
Figure 2. The variation of Probability density $|\Psi|^2$ with r and atomic number Z for 7s state (**a**), 8s state (**b**), 9s state (**c**) and 10s state (**d**) of free Hydrogen-like atoms.

number, for example the quantities in Table are calculated separately for cases of atomic number (*a*) $Z = Z_1$, (*b*) $Z = Z_2$ and then their respective differences are evaluated. These results are verified by Eqs. (19) and (20) and equal value of $\frac{Z_2}{Z_1}$ have equal $\delta S_\rho(Z)$ and $\delta S_\gamma(Z)$ but opposite to each other for each principal quantum number n. A negative value of $\delta S_\rho(Z)$ shows that the wavefunction and electron probability density in position space is compressed (localized) with increases of Z and which compress in a ratio equal to $\delta S_\rho(Z)$, shown in Figs. 1 and 2. The wavefunction and electron probability density in momentum space expands (delocalizes) with increases in Z and expands in a ratio equal to $\delta S_\gamma(Z)$ if $\delta S_\gamma(Z)$ is positive.

The variation (difference) in S_ρ and S_γ for cases of principal quantum number (*a*) n_1, (*b*) n_2 (holding Z constant) can be written as

$$S_\rho(n_2) - S_\rho(n_1) = \delta S_\rho(n) \approx \frac{23}{4}N\ln 2 \approx 4.0N \tag{21}$$

$$S_\gamma(n_2) - S_\gamma(n_1) = \delta S_\gamma(n) \approx -\frac{15}{4}N\ln 2 \approx -2.6N \tag{22}$$

where, $N = \log_2(n_2/n_1)$.

From Eqs. (21) and (22), we conclude that the variation of Shannon entropy with principal quantum number n is independent to Z and depends only to n_2/n_1 and also observe that the variation of Shannon entropy in position space S_ρ with n is not equal to the variation of Shannon entropy in momentum space S_γ with n for constant Z ($\delta S_\rho(n) \neq \delta S_\gamma(n)$). Increasing '$n$' results in the expansion of wavefunction in position space and compression of the wavefunction in momentum space but increase and decrease are not in the same ratio. Due to this, total Shannon entropy S_T doesn't remain constant with increase in n for constant Z. So, the variation of total Shannon entropy S_T with n for constant Z as $\delta S_T(n) = \delta S_\rho(n) + \delta S_\gamma(n) \approx 1.4N$. Positive sign of $\delta S_\rho(n)$ shows that S_ρ increases with increasing of n and negative sign of $\delta S_\gamma(n)$ show that S_γ decreases with increasing of n.

For the free system, we can describe S_ρ and S_γ as functions of Energy E and principal quantum number n, respectively.

$$S_\rho(n, E) \approx \frac{11}{4}\ln n - \frac{3}{2}\ln 2 + \ln\pi - \frac{3}{2}\ln(-E) + 3 \tag{23}$$

$$S_\gamma(n, E) \approx -\frac{3}{4}\ln n + \frac{13}{2}\ln 2 + 2\ln\pi + \frac{3}{2}\ln(-E) - \frac{10}{3} \tag{24}$$

Summing Eqs. (23) and (24) and we get total Shannon entropy

Z_1	Z_2	$X = \log_2(Z_2/Z_1)$	Analytical results		6s		7s		8s	
			$\delta S_\rho(Z)$	$\delta S_\gamma(Z)$	$\delta S_\rho(Z)$	$\delta S_\gamma(Z)$	$\delta S_\rho(Z)$	$\delta S_\gamma(Z)$	$\delta S_\rho(Z)$	$\delta S_\gamma(Z)$
0.5	1.0	1.0	− 2.079442	2.079442	− 2.079311	2.079306	− 2.079314	2.079252	− 2.079302	2.07882
	2.0	2.0	− 4.158883	4.158883	− 4.158565	4.158405	− 4.158602	4.158311	− 4.158632	4.158907
	3.0	2.584963	− 5.375278	5.375278	− 5.374876	5.374654	− 5.374882	5.37512	− 5.375046	5.378024
	4.0	3.0	− 6.238325	6.238325	− 6.237855	6.237575	− 6.237855	6.237751	− 6.237839	6.237515
1.0	2.0	1.0	− 2.079442	2.079442	− 2.079284	2.079099	− 2.079288	2.079059	− 2.07933	2.080087
	3.0	1.584963	− 3.295837	3.295837	− 3.295565	3.295348	− 3.295568	3.295868	− 3.295744	3.299204
	4.0	2.0	− 4.158883	4.158883	− 4.158544	4.158269	− 4.158541	4.158499	− 4.158537	4.158695
2.0	3.0	0.584963	− 1.216395	1.216395	− 1.216281	1.216249	− 1.21628	1.216809	− 1.216414	1.219117
	4.0	1.0	− 2.079442	2.079442	− 2.07926	2.07917	− 2.079253	2.07944	− 2.079207	2.078608
3.0	4.0	0.415037	− 0.863046	0.863046	− 0.862979	0.862921	− 0.862973	0.862631	− 0.862793	0.859491

Table 2. The analytical and numerical values of the variation (difference) of Shannon entropy in both position space and momentum space for cases of atomic number (*a*) Z_1, (*b*) Z_2.

$$S_T \approx 2\ln n + 5\ln 2 + 3\ln \pi - \frac{1}{3}, \tag{25}$$

Since total Shannon entropy, S_T is independent of energy E for constant n. Now, using Eqs. (23) and (24) we can write the variation (difference) in S_ρ and S_γ for cases of Energy (*a*) E_1, (*b*) E_2 (holding n constant) as

$$S_\rho(E_2) - S_\rho(E_1) = \delta S_\rho(E) = -\frac{3}{2}Y\ln 2 \approx -1.04Y \tag{26}$$

$$S_\gamma(E_2) - S_\gamma(E_1) = \delta S_\gamma(E) = \frac{3}{2}Y\ln 2 \approx 1.04Y \tag{27}$$

where, $Y = \log_2(\frac{E_2}{E_1})$.

From Eqs. (26) and (27), we conclude that the variation of Shannon entropy with E is also independent to principal quantum number n and depends only to $\frac{E_2}{E_1}$ and also observe that the variation of Shannon entropy in position space S_ρ with E is equal to negative of the variation of Shannon entropy in momentum space S_γ with E for constant n ($\delta S_\rho(E) = -\delta S_\gamma(E) \approx -1.04Y$). Negative sign of $\delta S_\rho(E)$ shows that S_ρ decreases with increasing of $\frac{E_2}{E_1}$ and positive sign of $\delta S_\gamma(E)$ show that S_γ increases with increasing of $\frac{E_2}{E_1}$. Due to this, total Shannon entropy S_T remains constant with changing in energy E for constant principal quantum number n.

Trapped linear Rydberg states. There have been numerous studies on trapped Rydberg states. In Fig. 3, we have plotted the variation of Shannon entropy in position space S_ρ and Shannon entropy momentum space S_γ as a function of confinement radius for trapped linear Rydberg states of hydrogen-like atoms. As shown in insets, the results are for five values of atomic number namely Z = 0.5, 1, 2, 3, and 4. Fig. (3(a)) represents for 7*s* states, (3(b)) for 8*s* states, (3(c)) for 9*s* states and (3(d)) for 10*s* states. We observe that for all *s* states the value of Shannon entropy in position space S_ρ decreases with increasing compression while Shannon entropy momentum space S_γ increases, which is as expected. As a result, we can say that as compression increases, the spatial wavefunction becomes more localized and the momentum wavefunction becomes more delocalized. Except for free atom(at large value of *r*), $\delta S_\rho/\delta r \neq -\delta S_\gamma/\delta r$ at each value of *r*. The Dirac-Fourier transform, which relates the densities in the position and momentum spaces differently under differently spatially confined spaces (different r), is the reason for this difference in the variation of two entropies[85]. Therefore, the total Shannon entropy $S_T = S_\rho + S_\gamma$ is not constant when *r* changes from the free atomic state ($r = \infty$) to 0. Total Shannon entropy S_T, corresponding to S_ρ and S_γ which are presented in Fig. 3, is displayed in Fig. 4. As in case of S_ρ and S_γ, the results of S_T are presented for five values of atomic number namely Z = 0.5, 1, 2, 3, and 4. The straight lines show the value of S_T for two extreme cases, one for free Hydrogen atom (FHA) and second for particle in a spherical box (PISB). Figure (4(a)) represents for 7*s* states, (4(b)) for 8*s* states, (4(c)) for 9*s* states and (4(d)) for 10*s* states. We observe that the total Shannon entropy S_T increases with increasing compression (*r* changes from ∞ to 0) and makes several peaks. Near tight confinement, S_T decreases with increasing more compression and becomes the equal particle in a spherical box (PISB) for each value of Z. Because there is an equal number of nodes in the wavefunction for each value of atomic number Z for constant principal quantum number n, so, there is an equal number of peaks in the total Shannon entropy S_T for each value of Z for constant principal quantum number n. But the position of each peak shifts to tight confinement with increasing the atomic number Z and it is inverse proportional to Z for constant n because the extension of the wavefunction decreases with the increasing the atomic number Z for constant principal quantum number n. But the height of each peak is independent of the atomic number Z for a constant principal quantum number n. The minimum value of the total Shannon entropy S_T equals S_T of the free hydrogen atom (FHA) for all values of Z. As a result, total Shannon entropy S_T for free atoms is unaffected by the atomic number Z, as discussed in the previous subsection. The maximum value of the total Shannon entropy S_T is the central peak which is nearest the critical radius (r_c). The critical radius is the characteristic radius of atoms, where the energy of atoms (E) becomes zero. And we have already discussed that
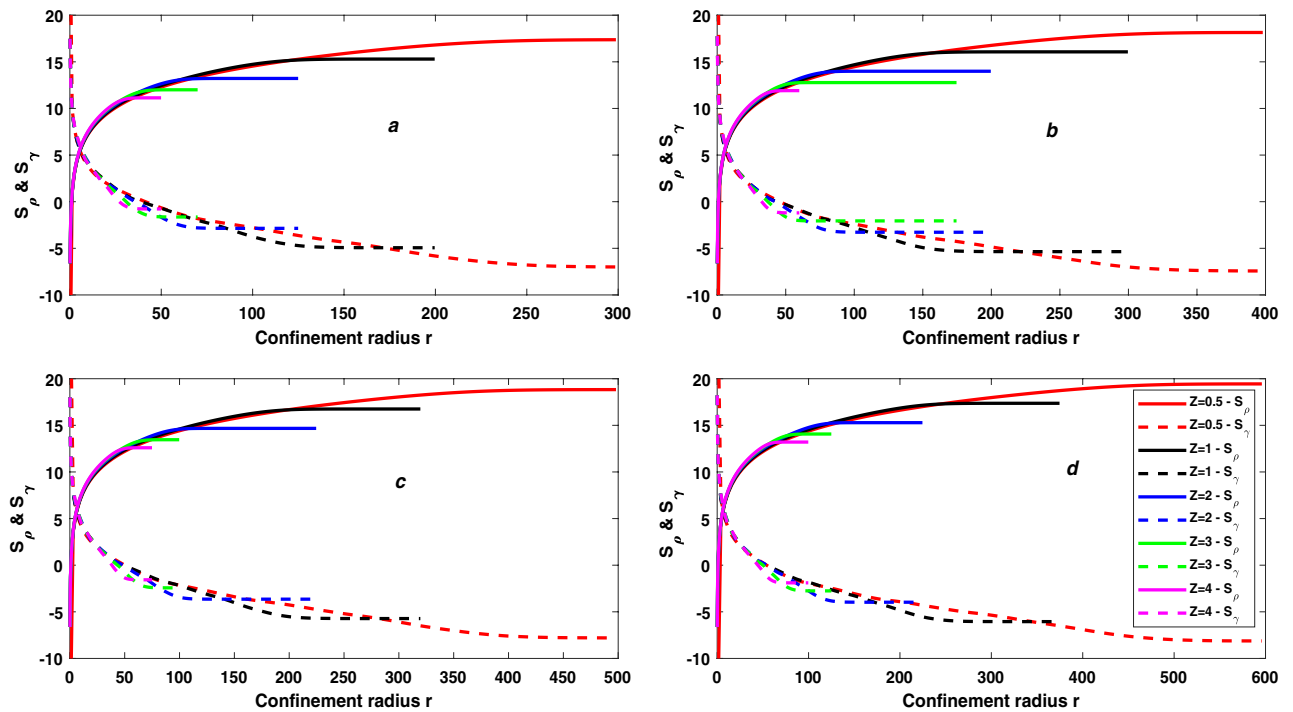
Figure 3. The variation of Shannon entropy in position space S_ρ and Shannon entropy in momentum space S_γ with confinement radius r and atomic number Z for 7s state (**a**), 8s state (**b**), 9s state (**c**) and 10s state (**d**) of trapped Hydrogen-like atoms.

height of the peak of S_T is independent of the atomic number Z for constant principal quantum number n, so we can say the maximum total Shannon entropy S_T is also independent of the atomic number Z for constant principal quantum number n. Also, there is an increasing number of nodes in wavefunction with increasing principal quantum number n. As a result, the number of peaks in the total Shannon entropy S_T increases in perfect agreement with the principal quantum number n. From Figs. 1 and 4, it is interesting that the number of peaks in the total Shannon entropy S_T is dependent on the number of nodes and they follow the relation

$$A = \frac{B}{2} = \frac{n-1}{2} \tag{28}$$

where, A = Number of peaks in S_T, B = Number of nodes in the wavefunction, and n principal quantum number.

So, we can say that the number of peaks in total Shannon entropy indicates the number of nodes in the wavefunction. But we know that extension of the wavefunction increases with increasing principal quantum number n. As a result, as the principal quantum number n increases, the position of each peak changes toward less confinement, while the atomic number Z remains constant. But the height of each peak increases with the increase of principal quantum number n for constant atomic number Z. So, the maximum total Shannon entropy S_T increases with the increase of principal quantum number n. However, for free atoms, the total Shannon entropy S_T is proportional to the principal quantum number n; as n increases, S_T increases, as stated in the previous subsection. So, we can say that the minimum S_T increases with increasing principal quantum number n in the same ratio of increase of the maximum S_T. Therefore, the difference between the maximum S_T and the minimum S_T is independent atomic number Z and principal quantum number n. From Fig. 4, the difference between maximum S_T and minimum S_T is always approximately 1.41 for confined linear states. However, the difference between the total Shannon entropy S_T corresponding to a particle in a spherical box (PISB) and a free Hydrogen atom (FHA) decreases as the principal quantum number n increases. The fact that the kinetic energy of the electron in FHA varies as $\frac{1}{n^2}$, while the kinetic energy of the electron in PISB is directly proportional to n^2, provides a rough approximation of states where the difference in total Shannon entropy S_T of PISB and FHA becomes almost zero. As a result, we expect these two entropies to equalize for $n \approx 15$ since the electron's kinetic energy is the same in both FHA and PISB for $n \approx 15$. This behavior of the total Shannon entropy in the CHA, PISB(no coulombic potential), and FHA(no confinement) is due to the effects of the Coulomb potential/confinement[86]. In Figure 5, we have plotted the variation of the product of variance in position space Δr and momentum space Δp (Heisenberg's Uncertainty) as a function of confinement radius for linear Rydberg states of confined hydrogen-like atoms. As shown in insets, the results are for five values of atomic number namely $Z = 0.5, 1, 2, 3,$ and 4. The straight lines show the value of $\Delta r \Delta p$ for two extreme cases, one for free Hydrogen atom (FHA) and second for particle in a spherical box (PISB). Figure (5(a)) represents for 7s states, (5(b)) for 8s states, (5(c)) for 9s states and (5(d)) for 10s states. We observe that $\Delta r \Delta p$ decreases with decreasing compression (r changes from 0 to ∞). Near high compression ($r \to 0$), $\Delta r \Delta p$ become the equal value of $\Delta r \Delta p$ of particle in a spherical box (PISB) for each value of Z. However, for free atom ($r \to \infty$), $\Delta r \Delta p$ becomes equal to the value for
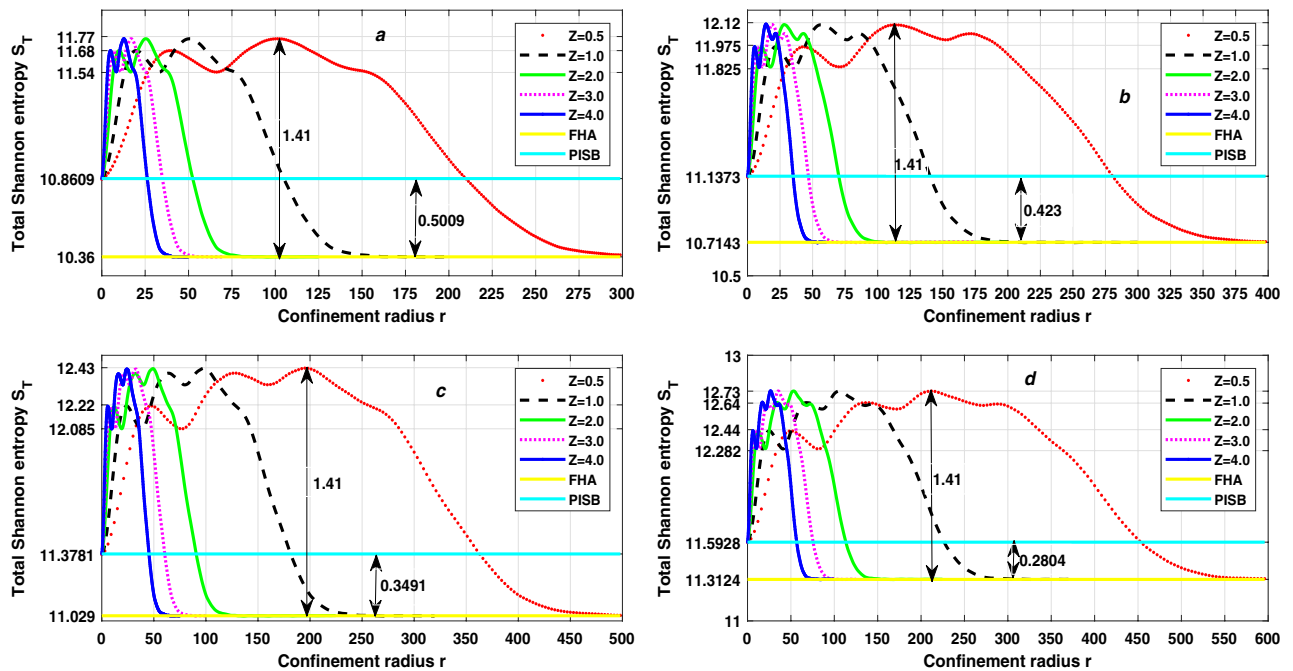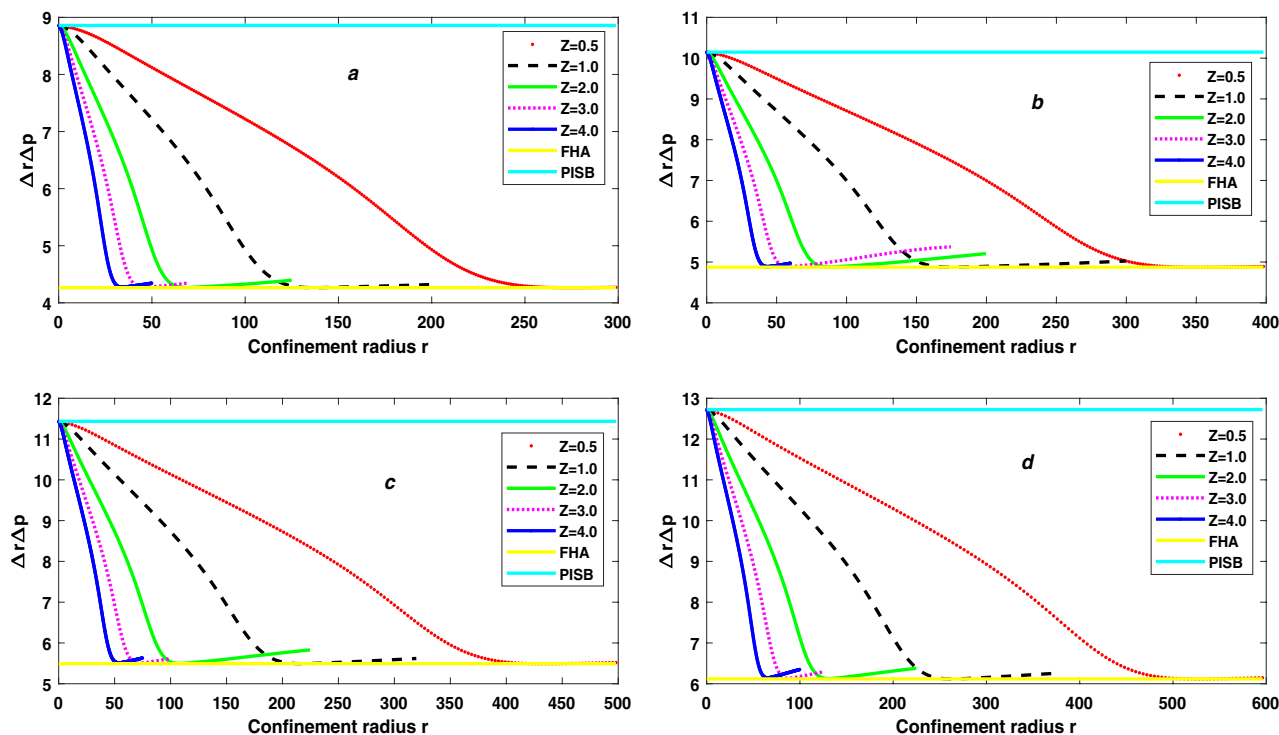
Figure 4. The variation of Total Shannon entropy S_T with confinement radius r and atomic number Z for 7s state (**a**), 8s state (**b**), 9s state (**c**) and 10s state (**d**) of trapped Hydrogen-like atoms.

free Hydrogen atom (FHA) for each value of Z. $\Delta r \Delta p$ increases as both the radius r and the atomic number Z of free atoms increase. So, Heisenberg's Uncertainty $\Delta r \Delta p$ is not constant with the atomic number Z for increasing the radius of free Rydberg atoms. However, uncertainty based on Shannon entropy is independent of the atomic number Z for free atoms for increasing the radius of free Rydberg atoms. Also, the number of nodes in the wavefunction does not affect $\Delta r \Delta p$. Hence, uncertainty relation based on Shannon entropy is superior to Heisenberg uncertainty for trapped Rydberg atoms.

Conclusion

In this work, the entropic measures like Shannon entropy in position and momentum spaces are presented for free and trapped Rydberg states of Hydrogen like atoms. We restricted our studies to principal quantum number ranging from 6 to 10. However, qualitative behaviour of these measures would reflect similar behaviour for higher excited states. We are able to compare the numerical values of Shannon entropy to analytical values for this system. We show that the total Shannon entropy S_T in case of linear Rydberg states is independent of atomic number Z and of course it is depends on n (principal quantum number). It is worth to mention that we have been able to show the measure of contraction (expansion) of wavefunction in terms of the difference of the Shannon entropies in respective spaces in terms of Z (atomic number) and n (principal quantum number). To the best of our knowledge this dependence of wavefunction localization (delocalization) in quantitative manner has not been reported so far. It is also shown that Shannon entropic uncertainty are better measure compare to Heisenberg Uncertainty relation for trapped Rydberg atoms. Finally, we understand that work presented here will provide useful information for further studies in trapped Rydberg species.

Figure 5. The variation of Heisenberg Uncertainty Principle $\Delta r \Delta p$ with confinement radius r and atomic number Z for 7s state (**a**), 8s state (**b**), 9s state (**c**) and 10s state (**d**) of trapped Hydrogen-like atoms.

References

1. Stebbings, R. F. & Dunning, F. B. *Rydberg States of Atoms and Molecules* (Cambridge University Press, 1983).
2. Gallagher, T. F. *Rydberg Atoms* (Cambridge University Press, 1994).
3. Jaksch, D. *et al.* Fast quantum gates for neutral atoms. *Phys. Rev. Lett.* **85**, 2208–2211 (2000).
4. Lukin, M. D. *et al.* Dipole blockade and quantum information processing in mesoscopic atomic ensembles. *Phys. Rev. Lett.* **87**, 037901 (2001).
5. Unanyan, R. G. & Fleischhauer, M. Efficient and robust entanglement generation in a many-particle system with resonant dipole-dipole interactions. *Phys. Rev. A* **66**, 032109 (2002).
6. Môller, D., Madsen, L. B. & Mòlmer, K. Quantum gates and multiparticle entanglement by Rydberg excitation blockade and adiabatic passage. *Phys. Rev. Lett.* **100**, 170504 (2008).
7. Möller, M., Lesanovsky, I., Weimer, H., Büchler, H. P. & Zoller, P. Mesoscopic Rydberg gate based on electromagnetically induced transparency. *Phys. Rev. Lett.* **102**, 170502 (2009).
8. Saffman, M. & Mòlmer, K. Efficient multiparticle entanglement via asymmetric Rydberg blockade. *Phys. Rev. Lett.* **102**, 240502 (2009).
9. Urban, E. *et al.* Observation of Rydberg blockade between two atoms. *Nature Phys.* **5**, 110–114 (2009).
10. Shao, Xiao-Qiang. Selective Rydberg pumping via strong dipole blockade. *Phys. Rev. A* **16**, 053118 (2020).
11. Madjarov, I. S. *et al.* High-fidelity entanglement and detection of alkaline-earth Rydberg atoms. *Nature Phys.* **16**, 857–861 (2020).
12. Bai, S. *et al.* Distinct antiblockade features of strongly interacting Rydberg atoms under a two-color weak excitation scheme. *New J. Phys.* **22**, 013004 (2020).
13. Carr, A. W. & Saffman, M. Preparation of entangled and antiferromagnetic states by dissipative Rydberg pumping. *Phys. Rev. Lett.* **111**, 033607 (2013).
14. Shao, Xiao-Qiang., You, Jia-Bin., Tai-Yu Zheng, C. HOh. & Zhang, Shou. Stationary three-dimensional entanglement via dissipative Rydberg pumping. *Phys. Rev. A* **89**, 052313 (2014).
15. Shi-Lei, Su., Guo, Qi., Wang, Hong-Fu. & Zhang, Shou. Simplified scheme for entanglement preparation with Rydberg pumping via dissipation. *Phys. Rev. A* **92**, 022328 (2015).
16. Walker, T. G. & Saffman, M. Consequences of Zeeman degeneracy for the van der Waals blockade between Rydberg atoms. *Phys. Rev. A* **77**, 032723 (2008).
17. Browaeys, A., Barredo, D. & Lahaye, T. Experimental investigations of dipole-dipole interactions between a few Rydberg atoms. *J. Phys. B Atmoic Mol. Opt. Phys.* **49**, 152001 (2016).
18. Browaeys, A. & Lahaye, T. Many-body physics with individually controlled Rydberg atoms. *Nature Phys.* **16**, 132–142 (2020).
19. Saffman, M. Quantum computing with atomic qubits and Rydberg interactions: progress and challenges. *J. Phys. B Atomic Mol. Opt. Phys.* **49**, 202001 (2016).
20. Zeng, Y. *et al.* Entangling two individual atoms of different isotopes via Rydberg blockade. *Phys. Rev. Lett.* **119**, 160502 (2017).
21. Bai, Z., Adams, C. S., Huang, G. & Li, W. Self-induced transparency in warm and strongly interacting Rydberg gases. *Phys. Rev. Lett.* **125**, 263605 (2020).
22. Wu, J. L. *et al.* Resilient quantum gates on periodically driven Rydberg atoms. *Phys. Rev. A* **103**, 012601 (2021).
23. Adams, C. S., Pritchard, J. D. & Shaffer, J. P. Rydberg atom quantum technologies. *J. Phys. B Atomic Mol. Opt. Phys.* **53**, 012002 (2020).

24. Michels, A., de Boer, J. & Bijl, A. Remarks concerning molecular interaction and their influence on the polarisability. *Physica* **4**, 981–994 (1937).
25. Dutta, S. K., Guest, J. R., Feldbaum, D., Walz-Flannigan, A. & Raithel, G. Ponderomotive optical lattice for Rydberg atoms. *Phys. Rev. Lett.* **85**, 5551–5554 (2000).
26. Saffman, M. & Walker, T. G. Analysis of a quantum logic device based on dipole-dipole interactions of optically trapped Rydberg atoms. *Phys. Rev. A* **72**, 022347 (2005).
27. Isenhower, L., Williams, W., Dally, A. & Saffman, M. Atom trapping in an interferometrically generated bottle beam trap. *Opt. Lett.* **34**, 1159–1161 (2009).
28. Anderson, S. E., Younge, K. C. & Raithel, G. Trapping Rydberg atoms in an optical lattice. *Phys. Rev. Lett.* **107**, 263001 (2011).
29. Zhang, S., Robicheaux, F. & Saffman, M. Magic-wavelength optical traps for Rydberg atoms. *Phys. Rev. A* **84**, 043408 (2011).
30. Anderson, D. A., Schwarzkopf, A., Sapiro, R. E. & Raithel, G. Production and trapping of cold circular Rydberg atoms. *Phys. Rev. A* **88**, 031401 (2013).
31. Schwarzkopf, A., Anderson, D. A., Thaicharoen, N. & Raithel, G. Spatial correlations between Rydberg atoms in an optical dipole trap. *Phys. Rev. A* **88**, 061406 (2013).
32. Cortiñas, R. G. *et al.* Laser trapping of circular Rydberg atoms. *Phys. Rev. Lett.* **124**, 123201 (2020).
33. Mashhadi, L. & Shayeganrad, G. *Localized Excitation of Single Atom to a Rydberg State with Structured Laser Beam for Quantum Information* (Quantum Electronic, IntechOpen, 2019).
34. Saffman, M., Walker, T. G. & Mølmer, K. Quantum information with Rydberg atoms. *Rev. Mod. Phys.* **82**, 2313–2363 (2010).
35. Zeng, Y. *et al.* Entangling two individual atoms of different isotopes via Rydberg blockade. *Phys. Rev. Lett.* **119**, 160502 (2017).
36. Kirova, T. *et al.* Strongly confined atomic localization by Rydberg coherent population trapping. *Opt. Lett.* **45**, 5440–5443 (2020).
37. Shannon, C. E. A mathematical theory of communication. *Bell Syst. Tech. J.* **27**, 379–423 (1948).
38. Nielsen, M. A. & Chuang, I. L. *Quantum Computation and Quantum information* (Cambridge University Press, Cambridge, 2010).
39. Maroulis, G., Sana, M. & Leroy, G. Molecular properties and basis set quality: an approach based on information theory. *Int. J. Quantum Chem.* **19**, 43–60 (1981).
40. Simas, A. M., Thakkar, A. J. & Simith, V. H. Jr. Basis set quality. II. Information theoretic appraisal of various s-orbitals. *Int. J. Quantum Chem.* **24**, 527–550 (1983).
41. Gadre, S. R., Sears, S. B., Chakravorty, S. J. & Bendale, R. D. Some novel characteristics of atomic information entropies. *Phys. Rev. A* **32**, 2602–2606 (1985).
42. Tripathi, A. N., Smith, V. H. Jr., Sagar, R. P. & Esquivel, R. O. Electron correlation in momentum space for the neon-atom isoelectronic sequence from F^- through Ar^{8+}. *Phys. Rev. A* **54**, 1877–1883 (1996).
43. Nagy, A. & Parr, R. G. Information entropy as a measure of the quality of an approximate electronic wave function. *Int. J. Quantum Chem.* **58**, 323–327 (1996).
44. Gadre, S. R. Information entropy and Thomas-Fermi theory. *Phys. Rev. A* **30**, 620–621 (1984).
45. Gadre, S. R. & Bendale, R. D. Maximization of atomic information-entropy sum in configuration and momentum spaces. *Int. J. Quantum Chem.* **28**, 311–314 (1985).
46. Karafiloglou, P. & Panos, C. P. Order of Coulomb and Fermi pairs: application in a π-system. *Chem. Phys. Lett.* **389**, 400–404 (2004).
47. Chen, Z., Wannere Corminboeuf, C. S., Puchta, R. & Schleyer, P. V. R. Nucleus-independent chemical shifts (NICS) as an aromaticity criterion. *Chem. Rev.* **105**, 3842–3888 (2005).
48. Tsallis, C. Possible generalization of Boltzmann-Gibbs statistics. *J. Stat. Phys.* **54**, 479–487 (1988).
49. Renyi, A. *Proc. 4th Symp. on Mathematics, Statistics and Probability* (Berkeley University Press, Berkeley, 1960).
50. Onicescu, O. Théorie de l'information énergie informationelle. *Comptes rendus de l'Academie des Sciences Series A-B* **263**, 841–842 (1966).
51. Huong, S., Chen, Z.-B. & Wu, S. Entropic uncertainty relations for general symmetric informationally complete positive operator-valued measures and mutually unbiased measurements. *Phys. Rev. A* **103**, 042205 (2021).
52. Romera, E., Sanchez-Moreno, P. & Dehesa, J. S. The Fisher information of single-particle systems with a central potential. *Chem. Phys. Lett.* **414**, 468–472 (2005).
53. Majumdar, S., Mukherjee, N. & Roy, A. K. Information entropy and complexity measure in generalized Kratzer potential. *Chem. Phys. Lett.* **716**, 257–264 (2019).
54. Sun, G. H. & Dong, S. H. Quantum information entropies of the eigenstates for a symmetrically trigonometric Rosen-Morse potential. *Phys. Scr.* **87**, 045003 (2013).
55. Abdelmonem, M. S., Afaf, A. H. & Nasser, I. Scaling behaviour of Fisher and Shannon entropies for the exponential-cosine screened coulomb potential. *Mol. Phys.* **115**, 1480–1492 (2017).
56. Beckner, W. Inequalities in Fourier Analysis. *Ann. Math.* **102**, 159–182 (1975).
57. Bialynicki-Birula, I. & Mycielski, J. Uncertainty relations for information entropy in wave mechanics. *Commun. Math. Phys.* **44**, 129–132 (1975).
58. Romera, E. & Dehesa, J. S. The Fisher-Shannon information plane, an electron correlation tool. *J. Chem. Phys.* **120**, 8906–8912 (2004).
59. Angulo, J. C., Antolin, J., Zarzo, A. & Cuchi, J. C. Maximum-entropy technique with logarithmic constraints: estimation of atomic radial densities. *Eur. Phys. J. D* **7**, 479–485 (1999).
60. Saha, S. & Jose, J. Shannon entropy as an indicator of correlation and relativistic effects in confined atoms. *Phys. Rev. A* **102**, 052824 (2020).
61. Yahya, W. A., Oyewumi, K. J. & Sen, K. D. Position and momentum information-theoretic measures of the pseudoharmonic potential. *Int. J. Quantum Chem.* **115**, 1543–1552 (2015).
62. Onate, C. A., Onyeaju, M. C., Ikot, A. N. & Ebomwonyi, O. Eigen solutions and entropic system for Hellmann potential in the presence of the Schrödinger equation. *Eur. Phys. J. Plus* **132**, 462 (2017).
63. Onate, C. A., Onyeaju, M. C., Abolarinwa, A. & Lukman, A. F. Analytical determination of theoretic quantities for multiple potential. *Sci. Rep.* **10**, 17542 (2020).
64. Kumar, K. & Prasad, V. Entropic measures of an atom confined in modified Hulthen potential. *Results Phys.* **21**, 103796 (2021).
65. Munjal, D., Sen, K. D. & Prasad, V. Shape effect on information theoretic measures of quantum heterostructures. *J. Phys. Commun.* **2**, 025002 (2018).
66. Olendski, O. Comparative analysis of information measures of the Dirichlet and Neumann two-dimensional quantum dots. *Int. J. Quantum Chem.* **121**, e26455 (2021).
67. Olendski, O. Quantum information measures of the Dirichlet and Neumann hyperspherical dots. *Eur. Phys. J. Plus* **136**, 390 (2021).
68. Mukherjee, N. & Roy, A. K. Information-entropic measures in free and confined hydrogen atom. *Int. J. Quantum Chem.* **118**, e25596 (2018).
69. Nascimento, W. S. & Prudente, F. V. Shannon entropy: a study of confined hydrogenic-like atoms. *Chem. Phys. Lett.* **691**, 401–407 (2018).
70. Sánchez, M. A. M., Vargas, R. & Garza, J. Shannon entropy for the hydrogen atom confined by four different potentials. *Quantum Rep.* **1**, 208–218 (2019).
71. Mukherjee, N. & Roy, A. K. Shell-confined atom and plasma: incidental degeneracy, metallic character, and information entropy. *Phys. Rev. A* **104**, 042803 (2021).

72. Salazar, S. J. C., Laguna, H. G., Dahiya, B., Prasad, V. & Sagar, R. P. Shannon information entropy sum of the confined hydrogenic atom under the influence of an electric field. *Eur. Phys. J. D* **75**, 127 (2021).
73. Dahiya, B., Kumar, K. & Prasad, V. Electric field modified quantum entropic measures of particle in a spherical box. *Eur. Phys. J. Plus* **136**, 1031 (2021).
74. Wang, D. *et al.* Entropic uncertainty relations for Markovian and non-Markovian processes under a structured bosonic reservoir. *Sci. Rep.* **7**, 1066 (2017).
75. Yang, Y. Y. *et al.* Dynamical characteristic of measurement uncertainty under Heisenberg spin models with Dzyaloshinskii-Moriya interactions. *Front. Phys.* **14**, 31601 (2019).
76. Chen, M. N., Wang, D. & Ye, L. Characterization of dynamical measurement's uncertainty in a two-qubit system coupled with bosonic reservoirs. *Phys. Lett. A* **383**, 977–984 (2019).
77. Ming, F. *et al.* Improved tripartite uncertainty relation with quantum memory. *Phys. Rev. A* **102**, 012206 (2020).
78. Wang, D., Ming, F., Song, X. K., Ye, L. & Chen, J. L. Entropic uncertainty relation in neutrino oscillations. *Eur. Phys. J. C* **80**, 800 (2020).
79. Rosa, S. L., Toranzo, I. V., Moreno, P. S. & Dehesa, J. S. Entropy and complexity analysis of hydrogenic Rydberg atoms. *J. Math. Phys.* **54**, 052109 (2013).
80. Yanez, R. J., Van Assche, W. & Dehesa, J. S. Position and momentum information entropies of the D-dimensional harmonic oscillator and hydrogen atom. *Phys. Rev. A* **50**, 3065–3079 (1994).
81. Dehesa, J. S., Martinez-Finkelshtein, A. & Sanchez-Ruiz, J. Quantum information entropies and orthogonal polynomials. *J. Comput. Appl. Math.* **133**, 23–46 (2001).
82. Patil, S. H., Sen, K. D., Watson, N. A. & Montgomery, H. E. Jr. Characteristic features of net information measures for constrained Coulomb potentials. *J. Phys. B Atomic Mol. Opt. Phys.* **40**, 2147–2162 (2007).
83. Jiao, L. G., Zan, L. R., Zhang, Y. Z. & Ho, Y. K. Benchmark values of Shannon entropy for spherically confined hydrogen atom. *Int. J. Quantum Chem.* **117**, e25375 (2017).
84. Guevara, N. L., Sagar, R. P. & Esquivel, R. O. Shannon-information entropy sum as a correlation measure in atomic systems. *Phys. Rev. A* **67**, 012507 (2003).
85. Sen, K. D. Characteristic features of Shannon information entropy of confined atoms. *J. Chem. Phys.* **123**, 074110 (2005).
86. Salazar, S. J. C., Laguna, H. G., Prasad, V. & Sagar, R. P. Shannon-information entropy sum in the confined hydrogenic atom. *Int. J. Quant. Chem.* **120**, e26188 (2020).

Author contributions

V.P. conceptualized, formulated the problem statement, wrote and revised final version of the manuscript. K.K. did computational work, analyzed the data and wrote intiial draft of the manuscript.

Competing interests

The authors declare no competing interests.

Additional information

Correspondence and requests for materials should be addressed to V.P.

Reprints and permissions information is available at www.nature.com/reprints.

Publisher's note Springer Nature remains neutral with regard to jurisdictional claims in published maps and institutional affiliations.